Springer

KSME

Journal of Mechanical Science and Technology 24 (11) (2010) 2241~2245
www.springerlink.com/content/1738-494x
DOI 10.1007/s12206-010-0815-4

Variable thermal loading analysis on (111) plane of single crystal gold †

Murugavel Rathinam*

College Advisor, Principal & Professor, King Institutions, TamilNadu, India

(Manuscript Received November 13, 2009; Revised March 7, 2010; Accepted July 14, 2010)

Abstract

The temperature response on the properties of single crystal gold (111) plane at elevated temperatures was considered in this work. The ability to perform nanoindentation experiments at elevated temperatures opens up significant new possibilities in nanotechnology. The experiments are performed at various temperatures of 373 K, 473 K and 573 K with tailor made Berkovitch tip of radius 100 nm to study the behavior of single crystal gold. The new phenomenon of material bouncing back under the indenter at the end of unloading was clearly noted, due to the accumulation of high energy. The results for different temperatures were compared. Our experiments clearly show the onset of the first burst of dislocation glide, which is indicated by a sudden increase of displacement with no increase of loading, the onset of plastic deformation in connection with the periodic bursts, and the strain hardening, softening and release effects. Pile up was also observed. The complete elastic range was found. There was significant drop in the hardness, elastic modulus and the increase in depth with increasing temperature. The elastic recovery was reduced at higher temperatures.

Keywords: Nanoindentation; Mechanical properties; Gold; Effect of temperature

1. Introduction

Materials behave differently in real-life environments due to unpredicted thermal loading conditions. Knowledge of the thermo-mechanical properties is relevant to industrial applications and high temperature nanoindentation is a promising technique for this purpose. Studies on the mechanical response of materials to nanoindentation on single crystals were not undertaken under different higher thermal loadings. Understanding the critical relationships between the temperature and mechanical properties of metals is very important in design and selecting suitable materials for real-life environments depending on the thermal loading.

Experimental work on Au (111) surface was performed [1]. Detailed explanation for the interpretation of scan line graph was given. The nanoindentation experimental results on Au (111), Au (110), and Au (100) were presented [2]. The yielding phenomenon is composed of series of discrete yielding events separated by elastic deformation. The onset of this behavior was in agreement with the calculations for the theoretical shear strength of gold. The results of experiments on point contact of gold were presented [3]. It was found that an atomistic pillar like elongated neck was formed by lattice slip and structural relaxation during retraction. Simulation on (111) surface of gold sample was done [4]. Indenter shape was spherical and the radius was 8 nm. The potential for the substrate was embedded atom method (EAM). The tip surface interaction was frictionless, and the indenter tip was represented by a repulsive potential. The substrate material, gold (Au), was represented by a slab of dimension 240x210x160A°, containing 470000 atoms. All of the defects in this system lie on {111} planes that are the energetically preferred slip planes in the FCC lattice. From the (111) surface, there are three unique {111} planes extending in to the bulk. In this structure, defects are seen parallel to only two of these three planes.

The indentation on (111) surface of gold sample was done by simulation [5]. The sample was 19 nm wide by 40 nm long by 12.5 nm thick. The indenter tip was spherical with a radius of 4 nm. The simulation temperature was 0 K. This paper explained that the dislocation mechanism was due to the release of compression beneath the indenter and due to the conservation of volume in the thin film during micro plastic deformation (bursts). This paper also explained that the rotation of the lattice during nanoindentation may account for the pile up. The first burst occurred when the maximum shear stress at the tip of the indenter reached the theoretical shear strength. The pile up also caused the change in slope of the indentation curve. The results of atomistic simulations to investigate the nanoindentation deformation properties of model nanocrystalline gold with grain diameters of 5 and 12 nm were presented [6]. It was found that the grain boundaries act as efficient sinks for dislocation nucleation below the indenter and the

† This paper was recommended for publication in revised form by Associate Editor Maenghyo Cho
* Corresponding author. Tel.: +91 4286 254252, Fax: +91 4286 243256
E-mail address: mrgvel@yahoo.com

intergranular sliding occurred. It was established that, at the 5 nm grain diameter regime there was a decrease in Young's modulus. The results of atomistic mechanisms of plastic deformation during nanoindentation of an Au (001) surface with a non-interacting indenter were presented [7]. The defect structures formed during the initial plastic yield were identified. While unloading the indenter after the first yield, the pressure due to compressive strain in the defect induced restoring forces that healed the plastic deformation. Also, they proposed a three step mechanism based on dislocation theory, which explained that the defects produced depended on the crystallography of the indented surface.

Experiments on single crystal ionic materials were performed [8]. Special attention was devoted to the elastic response before the onset of plastic yield. In-plane interactions played a key role in the indentation process performed with ultra sharp tips leading to a non Hertzian response of the elastic region of the nano-indentation curve. The results of mechanical property characterization of thin films using spherical tipped indenters were presented [9]. The use of very small spherical tipped indenters provided more tractable solution to the contact problem. The role of substrate and interface adhesion on the force-displacement behavior of thin films indented with spherical tipped indenters was also presented. The analytical formulation of the elastic limit that predicted the location and slip character of a homogeneously nucleated defect in crystalline metals was reported [10]. A fundamental framework for describing incipient plasticity that combined the results of atomistic, finite-element modeling, theoretical concepts of structural stability at finite strain, and experimental analysis was arrived at [11]. These findings provided a self-consistent explanation of the discontinuous elastic-plastic response in nanoindentation measurements, and a guide to fundamental studies across many disciplines that seek to quantify, predict the initiation and early stages of plasticity.

The advancements in making low dimensional structures from inorganic and organic compounds, determining the local properties and assembling complex structures were summarized [12]. The homogeneous nucleations of dislocations in dislocation-free single crystals were observed [13]. This was related to sudden jump in the force-displacement curve. The mechanical stress for the set-in of this pop-in effect was estimated with the Hertzian elastic contact theory. Experimental results of dislocation loop nucleation showed good agreement with the continuum theory of dislocations. The dislocations with a screw component were shown to glide across {111} planes and by a cross-slip mechanism giving rise to revolving terraces in the neighborhood of the nanoindentation trace with their edges parallel to compact <110> directions were found [14]. The molecular dynamics simulation results showed that the burst and arrest of stacking faults were the key factors for the plastic deformation of nanocrystalline copper under nanoindentation [15]. High temperature nanotesting by micro materials measuring technology explained the technique for higher temperature nanoindentation [16]. New high-temperature stages for small-scale mechanical property testing were described [17]. Nanoindentation results were presented for gold, soda-lime glass, fused silica and a polyimide. This research was focused on the bulk materials.

Small scale hardness and elastic modulus measurements on glass, gold, and single crystal silicon at room temperature and 473 K were performed [18]. The results showed that at 473 K the hardness and elastic modulus of soda lime glass and gold were lower than at room temperature. In contrast, indentation testing of Si (100) at 473 K produced a similar hardness value to that obtained at room temperature, although the modulus was again reduced, from 140.3 to 66.0 GPa. The value of hardness (H) was found to decrease when the displacement (h) was high as the temperature was increased, in line with the earlier results [19].

Research based on the analysis of materials as a function of temperature is limited and it was below 400 K. Also, it was limited to bulk materials. The temperature based experiments on single crystals and at higher temperature reaching nearly 600 K are at the initial stage. The unavailability of nanoindentation testing facility at these temperature levels made this possible. Due to the importance of such studies at elevated temperatures, we have initiated this innovative research on single crystals considering the operating conditions of the components at very high temperatures during various applications. It needs much research both by experiments and simulation to establish theory at elevated temperatures at the nanoscale.

The structural behavior and property changes during the thermal loading become equally important. This work attempts to explore the complete behavior of Au (111) at various temperatures, including the initial burst, the complete elastic recovery, the softening effect and the modulus and Hardness. In this experiment, the behavior of the single crystal gold (111) during loading and unloading are analyzed to understand the temperature effects during the loading and unloading cycle.

2. Experimental methodology

The experiments were performed with a tailor made Berkovitch tip of radius 100 nm. The sample temperatures of 373 K, 473 K and 573 K were considered. The testing facility and the specimen setup were as per the standard high temperature nanoindentation machine available for nanoindention testing. So the photographs of testing facility, specimen setup and specimen pictures were not taken.

Flat surfaces away from steps were chosen for nanoindentation by imaging the surface with atomic force microscope (AFM) at 7 x magnifications to locate a smooth and defect free surface. The sample surface was brought to a constant temperature for each experiment. Sample surface temperature was measured before the indentation. The loading rate was kept constant for different temperatures experiments.

The sample was 2 mm thick and 10 mm diameter. It takes

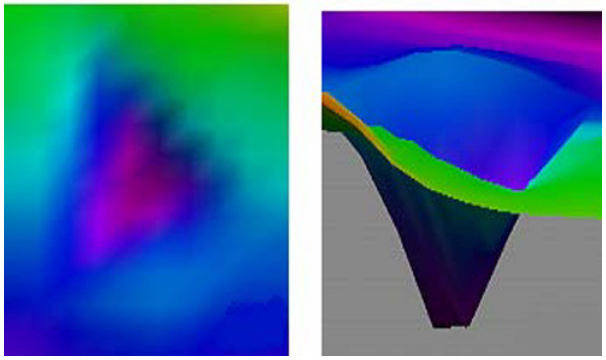

(a) (b)

Fig. 1. 3D view of sample after indentation at 4000x2500 nm (a) top view (b) side view showing hillock formation (pile up).

about 15 minutes to reach the required temperature. Imaging is done with 2 μN/s force. The topography and gradient images were taken to show the surface morphology after the indentation. In-situ imaging provides the capability to observe and quantify material damage while minimizing time for material recovery. The nanoindenter uses an area function based on the geometry of the tip, compensating for elastic load during the test. Use of this area function provides a method of gaining real-time nanohardness values from a load-displacement graph. Nanoindentation system allows the application of a specified force or displacement history, such that force, P, and the displacement, h, were controlled and/or measured simultaneously and continuously over a complete loading cycle using depth sensing indentation.

During the course of the instrumented indentation process, a record of the depth of penetration is made, and then the area of the indent is determined using the known geometry of the indentation tip. While indenting, various parameters such as load and depth of penetration can be measured. A record of these values can be plotted on a graph to create a load-displacement curve. These curves can be used to extract mechanical properties of the material. The hardness as the material is being indented resulting in hardness as a function of depth.

3. Results and discussion

Fig. 1(a) and 1(b) show the three-dimensional view of the sample after indentation. Fig. 1(a) shows the top view at 4000x2500 nm. A clearly visible striped pattern seen on the inside and outside of the surface of indentation may be due to the pressure on the adjacent vertical layers of material. Red color shows the two extreme regions of the sample after indentation and the patches of sky blue color around the indentation show the hillocks. Fig. 1(b) shows the penetration of the indenter in to sample. The figures are the directing imaging by the built in Atomic force microscope. The image is taken as the indenter penetrates the sample during the indentation process. This dynamic imaging from the AFM is an advantage in this experimental setup.

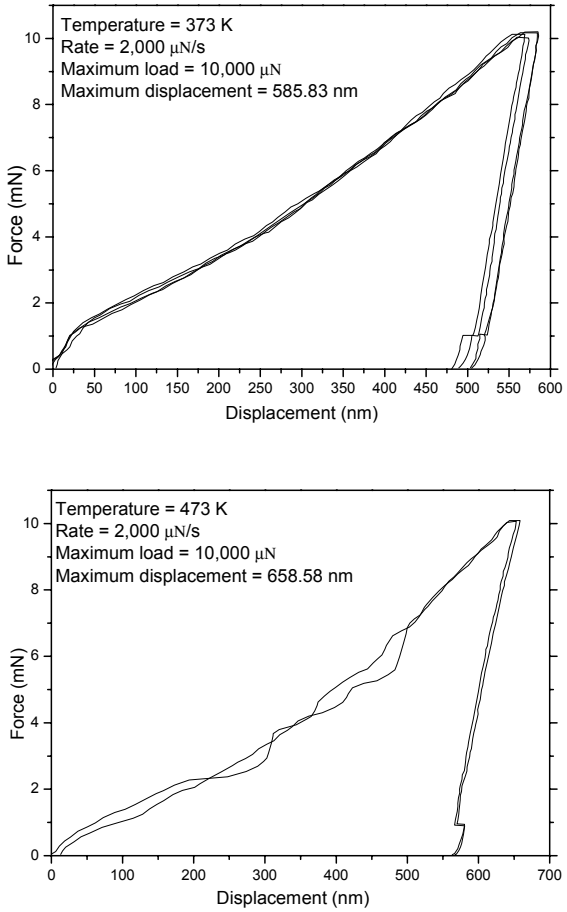

Fig. 2. Graph showing the loading and unloading pattern at 373 K and 473 K for 10,000 μN, 2000 μN/s.

Fig. 2 shows the plot of force vs. displacement at different temperatures revealing the temperature effects on the material. The loading rate is kept constant. The graph for 373 K and the graph at 473 K were compared. The maximum penetration depth is 585.83 nm at 373 K. From the graph, it clearly shown that the maximum depth is 658.58nm at 473 K.

It was clear from the penetration depths read from the curves that significant softening occurred at the higher temperatures. The softening effects were due to the increase in temperature and these softening effects produce increased plasticity. At high temperatures, the material is subjected to high plastic deformation. But it is a global deformation, instead of local burst causing the dislocations unlike the periodic burst (brittleness) in case of low temperature. The global deformation is the propagation of the damage throughout the sample. The exact data on the amount of softening will enable the proper selection of materials for different thermal loading conditions. The sudden burst at the end of unloading is noticed from the above graphs.

Fig. 3 shows the plot of force vs. displacement at a temperature of 573 K. It shows the softening effects as the penetration depth increases.

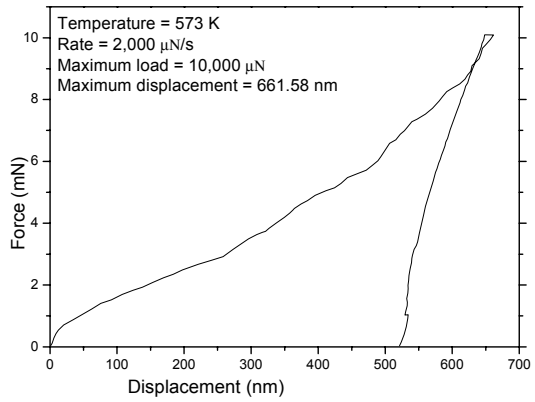

Fig. 3. Graph showing the loading and unloading pattern at 573 K for 10,000 μN, 2000 μN/s.

The graph corresponds to the sample temperature of 573 K. The penetration depth tends to increase in comparison to 473 K. From the graph, it is clear that the maximum penetration depth reaches 661.58 nm. But compared to 373 K and 473K, the change is small in case of 573 K. At high temperatures, the material was subjected to high plastic deformation. Increased recovery of the material is noted from the data based on maximum penetration depth and the maximum plastic region. In this case also, it is clear from the penetration depths read from the curves that significant softening occurred at the higher temperatures. The penetration depth reversal may be due to the strain hardening effects or hardening effects of the sample at this transition heating. But the penetration depth clearly changes from 373 to 473. Still we can see the increasing trend of the penetration depth. Only the plastic reverses. Hardness reverses revealing that there is some kind of mechanism operating during this transition. Some experiments were conducted on the experiment next day due to some reasons. So the temperature comes to room temperature and is heated again for further experiments. There may be some kind of hardening of the materials as it was heated, then cooled and then heated for some experiments.

Fig. 4 shows the relationship between force, time and displacement of the indenter of the indenter tip. It indicates the corresponding force and displacement with respect to the time during the indentation process.

From Table 1, it is noted that the difference between maximum plastic deformation ($h_{plastic}$) and maximum penetration depth (h_{max}) varies at different temperatures. In case of 373 K, it is about 52 nm. For 473 K, it is about 82 nm. For 573 K, it is 147 nm. This phenomenon shows that the plasticity range decreases as the temperature increases and penetration depth increases, causing a proportionate change in the plastic region indicating an increased failure of the material at high temperatures. The recovery of the material at high temperature is large. This material behaves more elastically as it is subjected to high temperature. The hardness decreases and displacement increases as the temperature increases. Also, it is noted that the value of elastic modulus (E) is inversely proportional to

Table 1. Comparison of data for different temperatures at 10,000 μN, 2000 μN/s.

Temp/constants	h_{max} nm	$h_{plastic}$ nm	H GPa	E GPa
373 K	584.13	528.22	1.28	42.58
	569.06	515.07	1.33	44.99
	573.94	518.42	1.31	43.14
	590.45	542.76	1.20	48.24
	585.83	535.73	1.25	47.03
473 K	653.18	569.14	1.1	26.10
	658.58	576.62	1.07	26.42
573 K	661.58	514.34	1.33	16.4

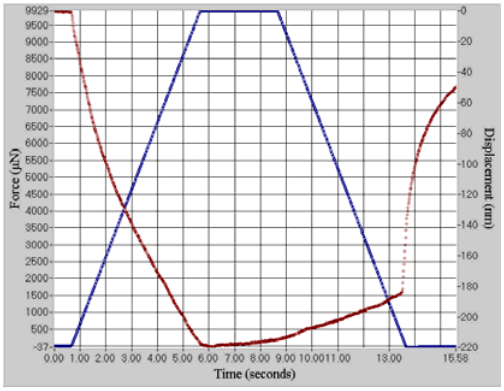

Fig. 4. The time, displacement, force curve during the indentation process.

the difference between $h_{plastic}$ and h_{max} and the hardness (H). The hardness (H) does not depend on this difference. The value of hardness (H) is found to decrease when the displacement (h) is high as the temperature increases in line with the results of Roger Smith et al.'s [19] results.

4. Conclusions

It is interesting to note that the curvature in the unloading curve has disappeared at the higher temperatures. This curvature is indicative of elastic recovery within the indentation itself. The elastic recovery of gold is small compared to other metals. This makes it an extreme case for modulus determination. From the difference in depth for different temperatures, it is found that there is significant increase in depth at higher temperature. This softening phenomenon corresponds to the increase of indentation depth at the constant loading conditions. The elastic recovery reduces at higher temperatures as the displacement increases, but the recovery of material with respect to the maximum displacement is large. The hardness for (111) orientation is higher compared to (110), as it is also found for Al. Jumps in the curves are observed at the end of unloading for higher loads. Possible causes may be the relocation of materials at the end of unloading, or phase transformation. The pop-ins shown by the *p-h* curves correspond to the formation of dislocations. The contact pressure (nanohardness)

increases with decreasing indentation depth. We attribute the temperature dependence to the increased dislocation mobility and the reduced dislocation density as the temperature increases. Pileup around an indentation is clearly observed. The onset of plastic deformation is identified from the periodic bursts. The new phenomenon of material under the indenter, bouncing back at the end of unloading was clearly noted. The hardness and elastic modulus also dropped at higher temperatures. It is noted that the plastic deformation is higher at higher temperatures. The softening of the material as the temperature increases would change the expected in-situ performance of a system causing malfunctioning. The set theory for these thermal variations is an important aspect in the design of materials for the system.

References

[1] J. D. Kiely, J. F. Jarausch, J. E. Houston and P. E. Russell, Initial stages of yield in nanoindentation, *J. Mater. Res*., 14 (1999) 2219-2227.

[2] S. G. Corcoran, R. J. Colton, E. T. Lilleodden and W. W. Gerberich, Anomalous plastic deformation at surfaces: Nanoindentation of gold single crystals Rapid Communications, *Phys. Rev. B*, 55 (1997) R16057-R16060.

[3] K. Tokushi, Atomic process of point contact in gold studied by time-resolved high-resolution transmission electron microscopy, *Phys. Rev. Lett*., 81 (1998) 4448-4451.

[4] C. L. Kelchner, S. J. Plimpton and J. C. Hamilton, Dislocation nucleation and the defect structure during surface indentation, *Phys. Rev. B*, 58 (1998) 11085-11088.

[5] J. A. Zimmerman, C. L. Kelchner, P. A. Klein, J. C. Hamilton and S. M. Foiles, Surface step effects on nanoindentation,*Phys. Rev. Lett*., 87 (2001) 165507-1-165507-4.

[6] D. Feichtinger, P. M. Derlet and H. Van Swygenhoven, Atomistic simulations of spherical indentations in nanocrystalline gold, *Phys. Rev. B*, 67 (2003) 024113-4.

[7] A. Gannepalli and S. K. Mallapragada, Atomistic studies of defect nucleation during nanoindentation of Au(001), *Phys. Rev. B*, 66 (2002) 104103-11.

[8] J. Fraxedas, S. Garcia Manyes, P. Gorostiza and F. Sanz, Nanoindentation: toward the sensing of atomic interactions, *PNAS*, 99 (2002) 5228-5232.

[9] M. V. Swain and J. Mencik, Mechanical property characterization of thin films using spherical tipped indenters, *Thin Solid Films*, 253 (1994) 204-211.

[10] Krystyn J. Van Vliet, Ju Li, Ting Zhu, S. Yip and S. Suresh, Quantifying the early stages of plasticity through nanoscale experiments and simulation, *Phys. Rev. B*, 67 (2003) 104105-15.

[11] J. L. Krystyn J. Van Vliet, Ting Zhu, S. Yip and S. Suresh, Atomistic mechanisms governing elastic limit and incipient plasticity in crystals, *Nature*, 418 (2002) 307-310.

[12] D. A. Bonnell, Materials in nanotechnology: New structures, new properties, new complexity*, J. Vac. Sci. Technol. A*, 21 (2003) S194-S206.

[13] D. Lorenz, A. Zeckzer, U. Hilpert, P. Grau, H. Johansen and H. S. Leipner, Pop-in effect as homogeneous nucleation of dislocations during nanoindentation, *Phys. Rev. B*, 67 (2003) 172101-4.

[14] E. Carrasco, O. Rodriguez de la Fuente, M. A. Gonzalez and J. M. Rojo, Dislocation cross slip and formation of terraces around nanoindentations in Au (001), *Phys. Rev. B*, 68 (2003) 180102-4.

[15] X.-L. Ma and W. Yang, Molecular dynamics simulation on burst and arrest of stacking faults in nanocrystalline Cu under nanoindentation, Nanotechnology, 14 (2003) 1208-1215.

[16] High temperature nanotesting, micro materials measuring nanotechnology-http://freespace.virgin.net/micro.materials/.

[17] B. D. Beake and J. F. Smith, High-temperature nanoindentation testing of fused silica and other materials, *Philosophical Magazine A*, 82 (2002) 2179-2186.

[18] J. F. Smith and S. Zhang, High temperature nanoscale mechanical property measurements, *Surface Engineering*, 16 (2000) 143-146.

[19] R. Smith, D. Christopher and S. D. Kenny, Defect generation and pileup of atoms during nanoindentation of Fe single crystals, *Phys. Rev. B*, 67 (2003) 245405-14.

Murugavel Rathinam received The Bachelor of Engineering (B.E) in Mechanical Engineering from University of Madras, India, in 1993. He then received the Master of engineering (M.E) in Engineering Design from Government College of Technology in 1997 and Ph.D. degree from The Hong Kong Polytechnic University, Hong Kong, in 2004. He served as a Senior Engineer (R&D) in TATA Engineering and Locomotive Company. He is a recipient of International Fellowship from Government of Hong Kong. He was awarded the excellent teacher award. Dr. Rathinam is currently a College Advisor & Professor at King Institutions, India. He has got over 16 years of experience in teaching, research and Industry. He has enormous international exposure in foreign Universities in many countries. He serves as an Editor & reviewer of International Journals and Books. Dr. Rathinam's interests include Nanotechnology, Design, Mechanics, Materials, Solid state electronics, innovative projects and Methodologies, Social, educational and administrative research.